Cellular and Molecular Life Sciences (2025) 82:100
https://doi.org/10.1007/s00018-025-05630-y

ORIGINAL ARTICLE

Nuclear translocation of CDK5RAP3 regulated by NXF3 promotes the progression of gastric cancer

Cheng Zhang[1] · Dongyang Wang[1] · Yuguang Shen[1] · Yuanruohan Zhang[1] · Jiahua Liu[1]

Received: 4 September 2024 / Revised: 22 January 2025 / Accepted: 17 February 2025

Abstract

Background Nuclear-cytoplasmic transport proteins (NCTPs) impact the transport of proteins and RNA molecules between the nucleus and cytoplasm in tumor cells, making them promising targets for cancer therapy. Currently, the molecular mechanism and function of Nuclear RNA export factor 3 (NXF3) in gastric cancer (GC) remains unclear.

Methods We used Univariate Cox regression analysis and LASSO regression analysis, Receiver Operating Characteristic (ROC) curves to construct and evaluate a NCTP prognosis risk scoring model (NCTP model). Moreover, we identified the key NCTP (NXF3) affecting GC through differential expression and prognosis analysis. Subsequently, we introduced NXF3 shRNA into GC cells to investigate the impact of NXF3 on the cell proliferation, cell migration, invasion, and cell cycle and apoptosis and tumor growth by CCK-8 assay, transwell, wound healing assay, Flow cytometry, and nude mice subcutaneous tumor in vitro *and* in vivo. Furthermore, we investigated the key molecules influenced by NXF3 through piRNA-Seq, RNA-Seq, RIP-Seq, IP-MS, and Nuclear-cytoplasmic transcriptomics.

Results We constructed a prognostic risk model related to 3 NCTPs, including NXF3, GLE1 and RANGAP. The NCTP model effectively predicts the prognosis of GC patients. The low-risk group exhibited a significantly higher overall survival rate than that of the high-risk group. Notably, NXF3 is identified as a crucial NCTP in GC, and its high expression is associated with poor prognosis of GC patients. Knocking down of NXF3 significantly inhibited the proliferation, invasion, migration, cell cycle, tumor growth and induced cell apoptosis of GC cells in vitro and in vivo. Mechanistically, NXF3 modulates the cell cycle, cellular senescence related oncogenic pathways via piRNA-target network. Specifically, our findings highlighted several piRNA-related signaling pathways in GC, such as piRNA_3457319-CCND1/CDKN1A-p53, piRNA_2847077-TGFB3/TGFBR2-Cellular senescence, piRNA_448895-IGF1/PDGFRA/ACTB/MAP2K6-Rap1. Moreover, NXF3 was shown to facilitate the nuclear export of CDK5RAP3 mRNA, thereby promoting cell cycle progression and increasing cancer cell proliferation in gastric cancer.

Conclusion Our study demonstrates that NXF3 modulates cell cycle progression and promotes gastric cancer development through piRNA-related pathways and the nuclear export of CDK5RAP3 mRNA. Targeting NXF3 represents a promising strategy for developing novel therapeutic approaches for gastric cancer.

Keywords Gastric cancer · Nuclear-cytoplasmic transport · NXF3 · Cell cycle · PiRNA · CDK5RAP3

Introduction

Gastric cancer (GC) stands as the fourth most prevalent cancer globally, characterized by high morbidity and mortality rates [1]. In 2022, an estimated 480,000 new GC cases are anticipated in China, constituting 45% of global cases, with an incidence rate of 10.5% [2]. Despite advancements in surgical, chemotherapeutic, targeted, and immunotherapeutic approaches, patients with advanced GC continue to face a bleak prognosis [3]. Hence, there is a critical need to identify key genes and therapeutic targets influencing GC prognosis.

✉ Jiahua Liu
18487182139@163.com; maxlau_9@126.com

[1] Department of Gastrointestinal Surgery, Renji Hospital Affiliated, Shanghai Jiaotong University School of Medicine, No.160, Pujian Road, Pudong New Area, Shanghai 200127, China

Published online: 03 March 2025

Nuclear-cytoplasmic transport proteins (NCTPs) play an important role in the occurrence and development of GC [4]. These proteins regulate the transport of protein and RNA molecules between the nucleus and cytoplasm, a process essential for maintaining cellular homeostasis and function [5]. The transport process is mainly mediated by the nuclear transport protein family, which consists of importins and exportins [6]. RAN, a key GTPase, is central to this transport process by providing the energy and directionality required for nucleocytoplasmic transport. RAN cycles between an active GTP-bound state in the nucleus and inactive GDP-bpund state in the cytoplasm. This cycling is crucial for the function of importins, which recognize nuclear localization signals (NLS) on cargo molecules and transport them into the nucleus, and exportins, which recognize nuclear export signals (NES) and transport cargo out of the nucleus. Dysregulation of nuclear transport protein expression or localization has been reported in many cancers, contributing to continuous proliferation of cancer cells, resistance to apoptosis, and immune evasion [7]. RAN was highly expressed in metastatic lymph nodes and has some predictive value for metastasis in GC. Ran promoted GC metastasis in vitro and in vivo via the importinβ/NF-κB/VEGF nuclear transport signaling pathway [8]. Nucleoporin 54(Nup54) induced CARM1 nuclear importation to promote gastric cancer cell proliferation and tumorigenesis through transcriptional activation and methylation of Notch2 [9]. Specific inhibitor of nuclear export (SINE) compounds inhibited gastric cancer cell proliferation, disrupted spheroid formation, induced apoptosis and halted cell cycle progression at the G1/S phase [10]. Therefore, disrupting the function of key nuclear-cytoplasmic transport proteins is a promising strategy for developing GC therapeutics.

Nuclear RNA export factor 3 (NXF3) is a member of the nuclear RNA export factor family that mediates the export of cellular mRNA from the nucleus to the cytoplasm for translation [11, 12]. NXF3 expression has been found to be increased in Hepatocellular carcinoma (HCC), and act as a prospective predictor of HCC prognosis [11]. However, the role of NXF3 in gastric cancer remains unclear. NXF3 is also known to mediate the transport of Piwi-interacting RNAs (piRNAs), which are small non-coding RNAs involved in gene silencing and regulation of genomic stability [13]. piRNAs are primarily known for their role in germ cells, but recent studies have implicated their involvement in cancer progression through regulation of oncogenic pathways. The canonical role of NXF3 is a germ cell-specific export adapter for un-spliced piRNA precursors, and involve in the transport process from transcription sites to cytoplasmic piRNA biogenesis sites [14]. However, the specific role of NXF3 and its regulation of piRNAs in gastric cancer progression remains to be determined.

CDK5RAP3 (CDK5 Regulatory Subunit-Associated Protein 3) is another key molecule involved in nucleocytoplasmic transport and cell cycle regulation. It has been implicated in various cellular processes, including cell proliferation, apoptosis, and DNA damage response [32]. Aberrant expression of CDK5RAP3 has been associated with poor prognosis in several cancers, suggesting its potential role as a tumor suppressor or oncogene depending on the context [33]. The interplay between NXF3 and CDK5RAP3 in the context of nucleocytoplasmic transport and gastric cancer progression is yet to be elucidated.

In the present study, we explored the potential role of NCTPs and developed prognosis -related NCTP model to assess prognosis value for GC patients using LASSO Cox regression. Next, we found Nuclear-cytoplasmic transport protein NXF3 affects the malignant characteristics of gastric cancer in vivo *and* in vitro. Mechanistically, we analyzed the effect of NXF3 on the transport of piRNAs and downstream target genes through RNA-Seq and piRNA-Seq analysis; on the other hand, we explored the nuclear translocation of mRNAs affected by NXF3 through RIP-Seq and Nuclear-cytoplasmic transcriptomics. This study first uncovers the role of NXF3 in gastric cancer, and targeting NXF3 suggests a promising strategy for GC therapeutics.

Material and methods

Data sources and preprocessing

TCGA datasets were downloaded from UCSC (https://xenabrowser.net/datapages/), including clinical data, count value

Table 1 Description of datasets used in the study

Dataset	Source	Sample size	Clinical characteristics	Inclusion criteria
TCGA-STAD	UCSC	n = 442	Gastric cancer tissues with corresponding clinical data (e.g., age, gender, survival)	Primary gastric adenocarcinoma samples with complete clinical and RNA sequencing data
GSE62254	GEO	n = 300	Gastric cancer tissues and adjacent normal tissues	Patients with histologically confirmed gastric cancer, with paired normal tissues
GSE84437	GEO	n = 224	Gastric cancer tissues and adjacent normal tissues	Patients with histologically confirmed gastric cancer, with paired normal tissues

and FPKM data. GSE62254 and GSE84437 were obtained from GEO. Description of Datasets was shown in Table 1. A set of 105 NCTPs were acquired from the KEGG pathway database (https://www.kegg.jp/kegg/pathway.html), with Nucleocytoplasmic transport item (ID 03013).

Establishment and validation of the NCTP related prognosis model

First, Univariate Cox regression analysis was used to identify prognosis-related NCTPs, with $P < 0.05$ considered to be associated with prognosis. LASSO is a compression method, and could more effectively deal with complex data, identify potential risk factors, and construct prognostic models [15]. LASSO penalty method was carried out using the "glmet" R package. Overall survival related NCTPs were fitted to LASSO regression model in TCGA-STAD dataset. The risk score of each patient's risk prognostic model (risk score = Σ expression * βi) was calculated by the coefficients from LASSO regression analysis and each gene expression level. A multifactor Cox model was built as follows: Risk score = (NXF3 expression × 0.037504) + (GLE1 expression × (−0.18981)) + (RANGAP1 expression × (−0.23789)). Each gastric cancer patient's risk score was calculated according to this prognosis risk model, and were classified into high-risk and low-risk groups based on the median value.

To evaluate the feasibility of the model, Kaplan–Meier analysis of high/low risk groups was implemented in TCGA-GC datasets, GSE62254 and GSE84437 datasets, respectively. The survival time of two groups were compared using "survival" R packages through Kaplan–Meier analysis. We used the "timeROC" R packages to create a time-dependent ROC curve. Univariate and multivariate Cox regression analysis were used to analyze whether the NCTPs-related prognostic model was independent of other clinical characteristics in predicting the prognosis of gastric patients.

Differential expression analysis of NCT genes

Using the "limma" R package for differential analysis, differentially expressed genes between adjacent tissues and gastric cancer tissues were identified, with the screening criteria set at log2|FC|> 1 and $P < 0.05$. Combining the 105 NCTPs obtained from the TCGA database, the corresponding NCT-related differentially expressed genes were obtained through intersection analysis. Subsequently, the intersection was taken with prognosis-related NCT genes identified through Univariate regression analysis, leading to the identification of the key nuclear-cytoplasmic transport gene NXF3 with consistent prognosis and expression trends.

Expression and prognostic analysis of NXF3, CDK5RAP3

The Human Protein Atlas (https://www.proteinatlas.org/) were used analyzed the protein expression of NXF3 in GC tissues sample. We utilized GEPIA (https://www.proteinatlas.org/) to compare the expression and prognostic significance of CDK5RAP3 in gastric cancer and adjacent tissues. The correlation between the expression of NXF3 and survival in GC were analyzed from Kaplan–Meier Plotter (https://kmplot.com/analysis/). Patients were divided into high-expression group and low-expression group based on NXF3 expression levels. Kaplan–Meier survival curves were plotted to demonstrate the difference in survival between the two groups of patients. The significance of the difference in survival curves was calculated using the log-rank test (P-value).

Cell culture

Gastric cancer cell lines (BGC-823 and AGS) and human gastric mucosal cells (GES-1) were obtained from the Institute of Cell Biology, affiliated with the Chinese Academy of Sciences (Shanghai, China).

The shRNA sequences for NXF3 were purchased from Hangzhou GuanNan Biotechnology Co., LTD. For cell transfection, BGC-823 and AGS were transfected with NXF3 shRNA1 (5'- CCGGCCTATACTATTTCACCCTAT ACTCGAGTATAGGGTGAAATAGTATAGGTTTTTG −3'), NXF3 shRNA2 (5'- CCGGCCAGAGCAACTTTA TGTGGTACTCGAGTACCACATAAAGTTGCTCTGGTT TTTG −3') and NXF3 shRNA3 (5'- CCGGACAAGCTC TTTGTGCGGGATACTCGAGTATCCCGCACAAAGAGC TTGTTTTTTG −3') using Lipofectamine™ 3000 (Invitrogen, MA, USA). As a result, RT-qPCR assays and Western blot assays indicated that shRNA2 displayed the most significant efficiency for NXF3 knockdown among BGC-823 and AGS cells.

Plasmid constructions

ShRNA2 sequences for NXF3 was constructed into pLKO.1-puro vector. ShRNA2 sequences used to establish a conditional BCG-823 and AGS silent cell line were constructed into Tet-pLKO-puro plasmid. Overexpression sequences for CDK5RAP3 was constructed into pCDH-CMV-Puro vector.

Establishment of stable cell lines

Constructed overexpression and silencing plasmids were transfected into 293 T cells by using Transfection Reagent Lipofectamine 2000(Invitrogen). After transfection, the supernatant containing lentivirus was collected, filter out

cell debris through a 0.45 μm filter membrane, and concentrate the virus particles by ultracentrifugation. Use the supernatant containing lentivirus was used to infect BCG-823 and AGS cells, adding polybrene (8 μg/ml) to enhance infection efficiency. After 48 h of infection, stably transfected cells were selected by using culture medium containing puromycin (2 μg/ml). The antibiotic-containing culture medium was added and cultured for 1–2 weeks to obtain stable transfected cell lines.

RT-qPCR assay

Total RNA was extracted from AGS, and BGC-823 cells using TRIzol reagent (Invitrogen, CA, USA). The isolated RNA was converted to cDNA using a reverse transcription kit (TaKaRa, Shanghai, China). Next, RT-qPCR assay was performed on an ABI 7500 PCR system using SYBR qPCR Master Mix (TaKaRa, Shanghai, China). The cycling parameters consisted of 45 cycles at 95 °C for 15 s, 55–60 °C for 15 s, and 72 °C for 15 s. The $2^{-\Delta\Delta Ct}$ method was needed to calculate relative expression levels in GC cell lines. The primer sequences for genes analyzed in this study are listed in Table 2.

Western blot assay

To validate the transfection efficiency of NXF3 knockdown and CDK5RAP3 overexpression (OE), we performed Western blot analysis. Total protein was extracted from BGC-823 and AGS cells using RIPA buffer (Beyotime, China). The protein concentration was measured using BCA assay kit (Thermo Fisher Scientific, USA). Equal amounts of protein were separated by SDS-PAGE and transferred to PVDF membranes (Millipore, USA). The membranes were blocked with 5% non-fat milk in TBST for 1 h at room temperature and then incubated with an anti-NXF3 primary antibody (1:1000, Proteintech, wuhan, China), CDK5RAP3 (1:1000, Proteintech, Wuhan, China) overnight at 4℃. After washing with TBST, the membranes were incubated with horseradish peroxidase-conjugated secondary antibody (1:5000, Proteintech, wuhan, China) for 1 h at room temperature. The protein bands were viaualized using an ECL detection kit (Thermo Fisher Scientific, USA).

Table 2 The primer sequences for the genes analyzed in this study

Gene symbol	Primer sequence (5'−3')
NXF3	Forward: CCGGCCTATACTATTTCACCCTAT
	Reverse: CCGGACAAGCTCTTTGTGCGGGAT
CDK5RAP3	Forward: GCTGCTGCTGCTGCTGCTGCT
	Reverse: CCTCCTCCTCCTCCTCCTCCT
CCND1	Forward: GAGGAGGAGGAGGAGGAGGAG
	Reverse: CTCCTCCTCCTCCTCCTCCT
CDKN1A	Forward: GCGCGCGCGCGCGCGCGCGC
	Reverse: GAGAGAGAGAGAGAGAGAGAG
CDKN3	Forward: TGGAGGAGGAGGAGGAGGAG
	Reverse: CTGCTGCTGCTGCTGCTGCT
GAPDH	Forward: GAGTCAACGGATTTGGTCGT
	Reverse: GACAAGCTTCCCGTTCTCAG

Cell proliferation and apoptosis assay

Cells were seeded in a 96-well plate at a density of 1500 cells per well. Cell counting kit-8 (Beyotime, Shanghai, China) was used to detect the cell proliferation after transfection. Cell apoptosis was detected by using the Annexin V-FITC/PI apoptosis detection kit (BD Biosciences, Franklin Lakes, USA).

Cell invasion and migration assay

For cell invasion assay, chamber inserts were added Matrigel (BD Biosciences, Franklin Lakes, USA)). Next, 1×10^5 cells were placed in the top chamber and incubated for 24 h. The chamber was then removed and fixed with 10% neutral formalin. Non-invasive cells were wiped off the membrane with a cotton swab, while the invading cells were stained with crystal violet for 20 min.

For the wound healing assay, a pipette tip was used to scratch the monolayer, after which the scratched cells were washed with PBS. Cell migration was monitored under the microscope and photographed at both 0 and 48 h. All assays were repeated at least three times.

Cell cycle detection

Cells are collected and washed in PBS (phosphate-buffered saline) to remove the culture medium or other impurities. The cells are fixed in pre-cooled 70% ethanol, typically fixed at 4 °C for 30 min to overnight. Cells are washed twice with PBS to remove the fixative, and the supernatant is removed by centrifugation. RNase is added to digest RNA to prevent non-specific binding of RNA with propidium iodide (PI) dye. PI dye is added for DNA staining. PI is a fluorescent dye that binds to DNA and produces a fluorescent signal, which is proportional to the DNA content. The stained cells are then analyzed using a flow cytometer. The fluorescence signal of PI is analyzed using flow cytometry software, typically detecting PE (Phycoerythrin) fluorescence in the FL-4-A channel or similar, to identify cells in different phases (G1, S, G2/M) based on the distribution of DNA content. Quantitative analysis of the percentage of cells in each phase can be done by manually setting thresholds or using software algorithms to fit Gaussian curves.

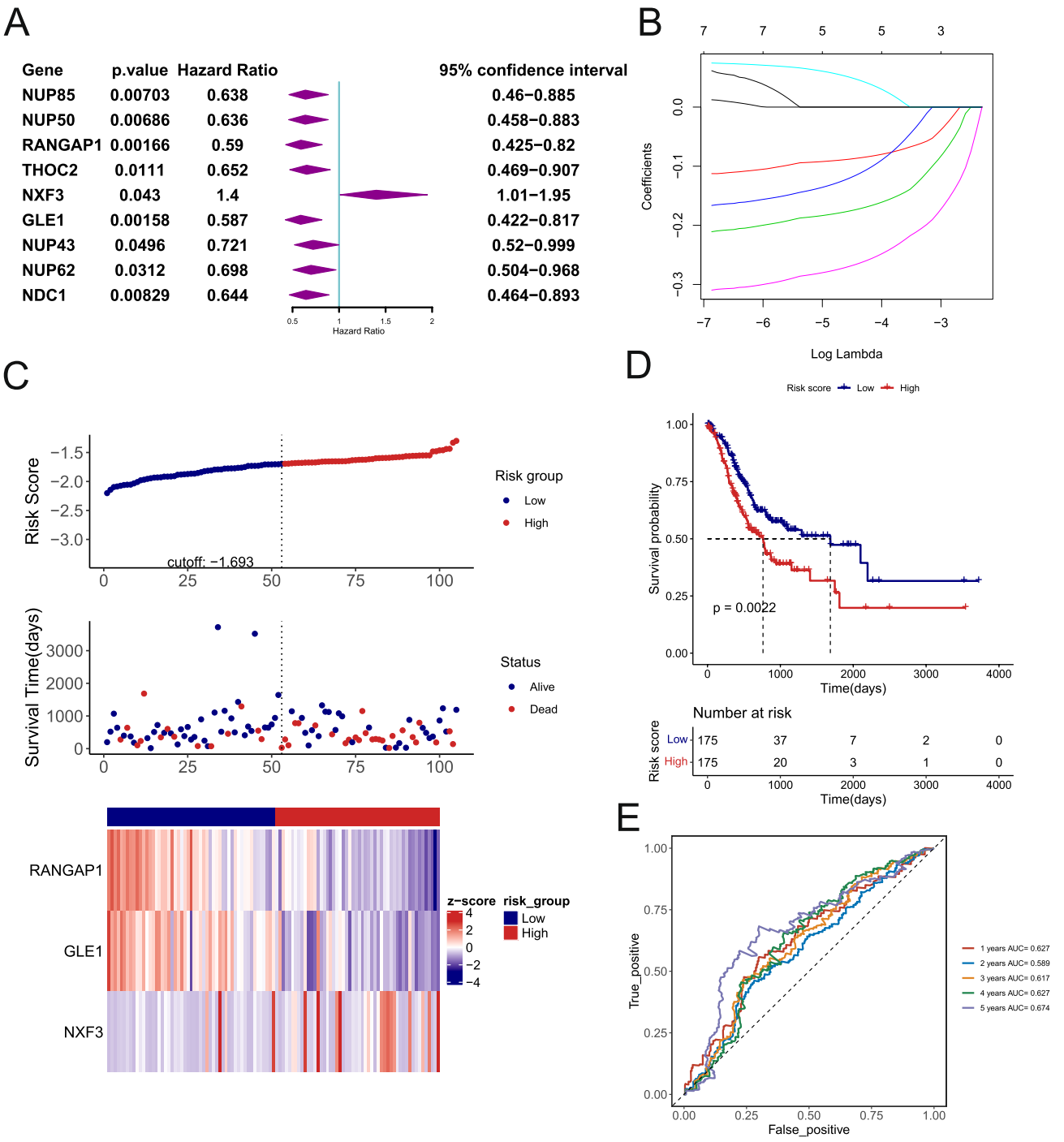

Figure1 Construction of NCTPs related prognosis risk model in gastric cancer. **A** NCTPs significantly associated with the prognosis of gastric cancer patients in Univariate analysis. **B** LASSO regression coefficient path diagram; **C** Overall survival score and overall survival status, heat map of NCTPs expression; **D** Survival curves of high-risk and low-risk group patients; **E** ROC curves of OS at 1, 2, 3, 4, and 5 years for gastric cancer patients

Nude mice xenograft model

All animal experiments conducted in this study were approved by the Laboratory Animal Care and Ethics Committee of Shanghai Jiaotong University. Male nude BALB/c mice at the age of 24 weeks were randomly divided into two groups (n = 5 per group), and subcutaneously injected with 5×10^6 shRNA-NXF3 BGC-823 cells

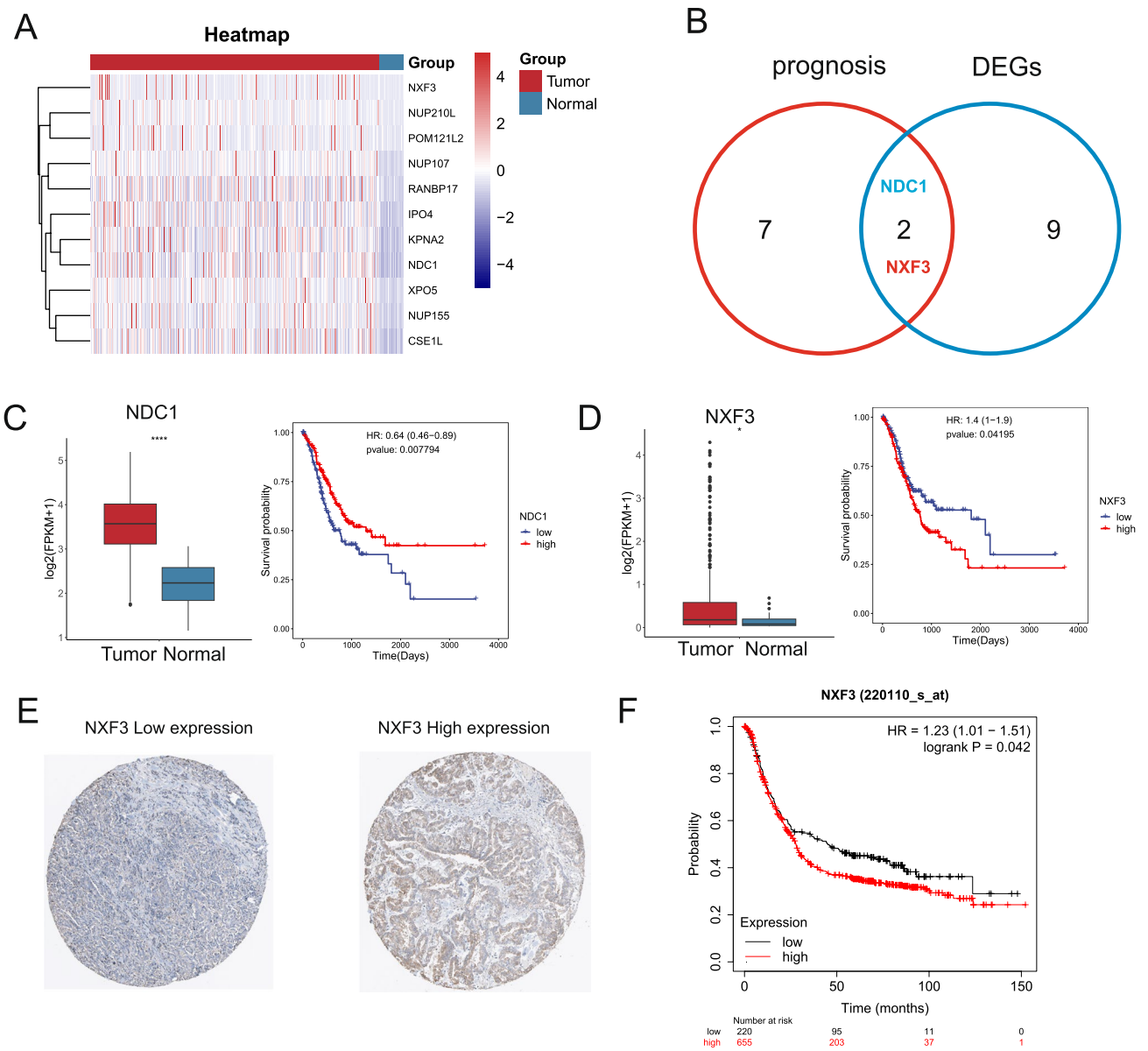

Fig. 2 High expression of NXF3 is associated with poor prognosis in gastric cancer. **A** Heatmap showing differentially expressed NCTPs in gastric cancer and adjacent tissues; **B** Venn diagram showing the intersection of DEGs related NCT and NCTPs associated with prognosis; **C** Differential expression and prognosis of NDC1 in gastric cancer and adjacent tissues; **D** Differential expression and prognosis of NXF3 in gastric cancer and adjacent tissues; **E** IHC assay showed that NXF3 low expression and NXF3 high expression in GC tissues from Human Protein Atlas (https://www.proteinatlas.org/) F The survival curve of GC patients for NXF3 low and NXF3 high expression from Kaplan–Meier Plotter dataset * $P < 0.05$, **** $P < 0.0001$.

(shNXF3 group) and vector BGC-823 cells (NC group). Mice were continuously monitored for their health condition and tumor growth. Once tumors began to grow on their backs, tumor size was measured using a ruler every 3 days to plot a tumor growth curve. The formula for calculating tumor volume is: V (mm^3) = ($a \times b^2$)/2, where "a" represents the tumor's maximum diameter and "b" represents the vertical height of the tumor. When the subcutaneously transplanted tumor reached a certain volume (generally with a maximum diameter not exceeding 2 cm), the mice were euthanized humanely, and the tumor tissue was collected and weighed.

Rna-sequencing and analysis

Total RNA was extracted from AGS-823 cells, with and without silenced NXF3, using the TRIzol reagent following

Table 3 Multivariate cox regression analysis of prognostic factor in GC patients

Variable	P value	Hazard_Ratio	Confidence_interval
NXF3 high	0.0397	1.43	1.185–2.09
Age > 60	0.034	1.57	1.03–2.37
Gender female	0.0885	0.699	0.463–1.06
Number_of_lymph-nodes_positive_by_he > 3	0.037	1.67	1.03–2.71
M M1	0.0076	2.52	1.28–4.95
N N1-3	0.561	1.21	0.631–2.34
T T3-4	0.768	1.08	0.634–1.85
Stage stage III-IV	0.756	1.11	0.572–2.16

standard procedures. The mRNA-Seq library was prepared. The library sequencing was performed, and the raw data were deposited. Differential gene criteria were set at $P\ value < 0.05$ and |Foldchange|> 1.2.

For Nuclear-cytoplasmic separation and RNA-Seq, nuclear-cytoplasmic separation reagent kit (Cat.78833, Thermo scientific, USA) was used to separate the nuclei and cytoplasm of cells in each group. Cells was collected and centrifuged after treatment with trypsin–EDTA. Wash cells with PBS, transfer cells to a micro-centrifuge tube and centrifuge. The supernatant was removed and dried the cell pellet as much as possible. Add cold CERI to the cell pellet. Centrifuge and transfer the supernatant (cytoplasmic extract). Resuspend the nuclear pellet with cold NER, centrifuge and transfer the supernatant (nuclear extract). RNA from the nuclei and cytoplasm was extracted, and then proceed with the following steps as described above.

Immunoprecipitation followed by mass spectrometry (IP-MS)

Proteins are extracted from cells in each group, and NXF3 and IgG antibodies are mixed separately with the proteins in the samples. The protein-antibody mixtures are then subjected to immunoprecipitation using protein A/G agarose or magnetic beads. The immunoprecipitated complexes are washed multiple times with washing buffer to remove non-specifically bound proteins. The target proteins are eluted from the immunoprecipitated complexes using appropriate elution buffer. The eluted proteins are digested with trypsin to generate peptide fragments. The digested peptide fragments are analyzed using a mass spectrometer. The mass spectrometer can determine the sequence and identification of the peptides based on their mass and charge.

RNA immunoprecipitation assay (RIP) and sequencing

RIP-Seq is a method that combines RNA immunoprecipitation (RIP) and next-generation sequencing to study the interactions between RNA and proteins. After collecting AGS cells, the cells were treated with RNase-free lysis buffer to release RNA–protein complexes. RNase-free protease inhibitors were added to the lysis buffer to prevent protein degradation. The lysate was centrifuged to remove undissolved cell fragments and insoluble substances, and the supernatant was retained for further experiments. The collected AGS cell lysate was divided into Input group, IgG group, and NXF3 group. Using the input sample as a control, in the NXF3 group, NXF3-specific antibodies and Protein A/G magnetic beads were added and co-incubated for 1 h; in the IgG group, IgG antibodies and Protein A/G magnetic beads were added and co-incubated for 1 h. Subsequently, the beads were washed multiple times with pre-chilled washing buffer PBS to remove non-specifically bound proteins and RNA. RNA was extracted from the eluate using RNA extraction reagent (Trizol reagent) and further purified through ethanol precipitation or column purification methods. The extracted RNA was converted into cDNA libraries following the standard RNA-seq library construction process on a high-throughput sequencing platform (Illumina platform). The constructed cDNA libraries were subjected to high-throughput sequencing to generate a large number of short sequences reads. The sequencing data were subjected to quality control and removal of low-quality reads and adapter sequences using Trimmomatic (version: 0.39). STAR (version: 2.7.3a) was utilized to align the clean reads to the human genome GRCh38. MACS2 (version 2.2.7.1) was used to detect peaks from the alignments under the option of -nomodel, with a q-value cutoff set at 0.05.

KEGG and GO function enrichment analysis

To investigate the functional and pathway enrichment of DEGs, Gene ontology (GO) and Kyoto encyclopedia of genes and genomes (KEGG) for DEGs were performed using the R package "clusterprofiler". GO enrichment analysis included the categories of Biological Process (BP), Cellular Component (CC), and Molecular Function (MF). The significance of each GO term was assessed by calculating p-values, with terms having p-values < 0.05 considered significantly enriched. Additionally, we employed the "enrichplot" package to generate bar plots. We utilized the "GOplot" package to calculate the z-score for each enriched term and visualize the GO and KEGG enrichment results. Additionally, we employed "ggplot2" packages to generate bar charts, further enhancing the readability of the results.

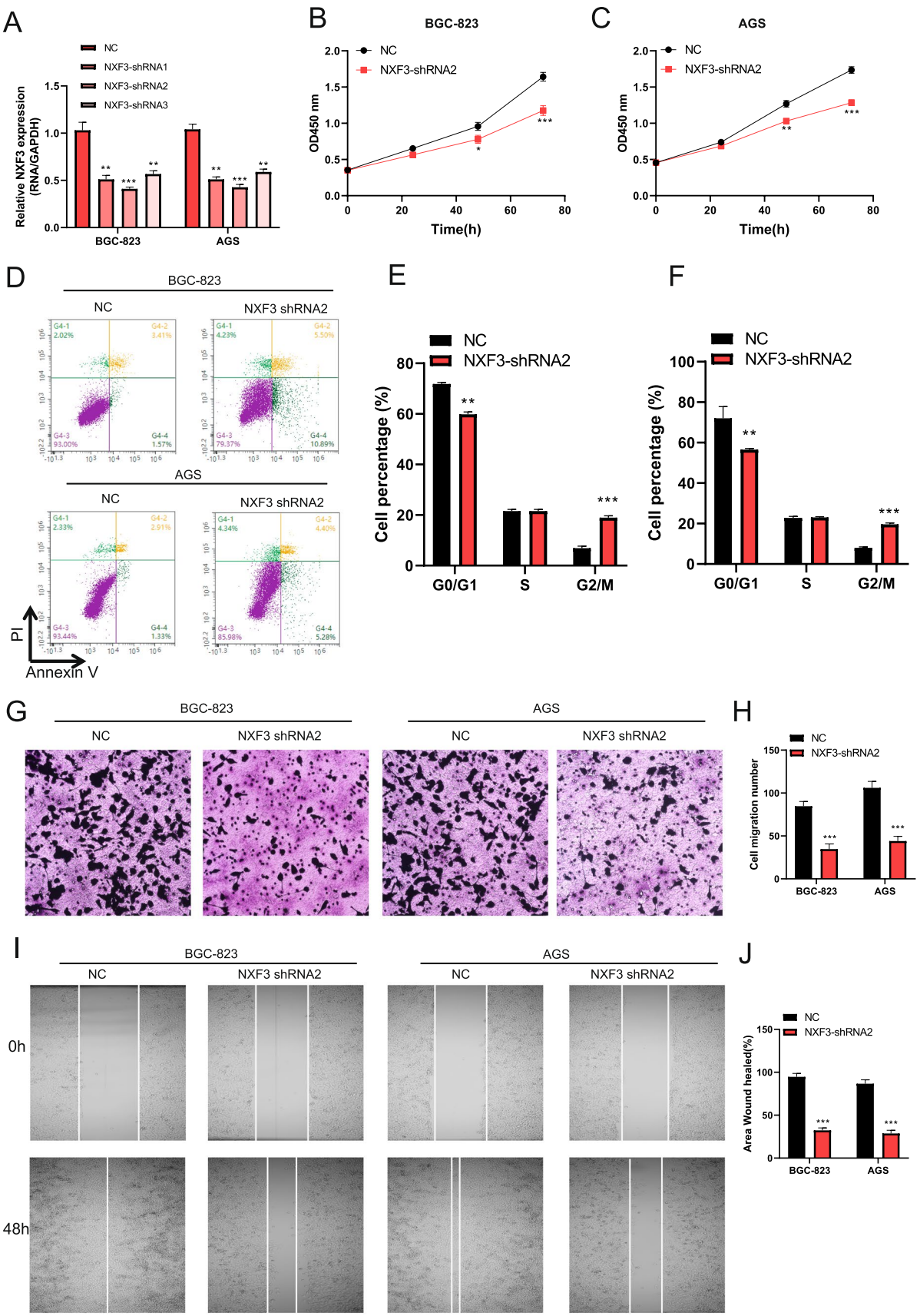
A
NC
NXF3-shRNA1
NXF3-shRNA2
NXF3-shRNA3
Relative NXF3 expression (RNA/GAPDH)
BGC-823
AGS
B
BGC-823
NC
NXF3-shRNA2
OD450 nm
Time(h)
C
AGS
NC
NXF3-shRNA2
OD450 nm
Time(h)
D
BGC-823
NC
NXF3 shRNA2
AGS
NC
NXF3 shRNA2
PI
Annexin V
E
NC
NXF3-shRNA2
Cell percentage (%)
G0/G1
S
G2/M
F
NC
NXF3-shRNA2
Cell percentage (%)
G0/G1
S
G2/M
G
BGC-823
NC
NXF3 shRNA2
AGS
NC
NXF3 shRNA2
H
NC
NXF3-shRNA2
Cell migration number
BGC-823
AGS
I
BGC-823
NC
NXF3 shRNA2
AGS
NC
NXF3 shRNA2
0h
48h
J
NC
NXF3-shRNA2
Area Wound healed(%)
BGC-823
AGS

◂**Fig. 3** NXF3 acts as an oncogene in vitro. **A** The transfection efficiency of NXF3 shRNA-1, −2, −3 were validated through RT-qPCR experiments. **B**-**C** CCK-8 assay was used to explore the effect of NXF3 shRNA2 on the proliferation of BGC-823 (**B**) and AGS cells (**C**). (**D**) Flow cytometry assay was used to verify the effect NXF3 shRNA2 on the apoptosis of BGC-823 and AGS cells. **E**–**F** Cell cycle detection after silencing NXF3 in BCG-823 and AGS cells; analysis of the proportion of cells in G0/G1 phase, S phase, and G2/M phase; (**G**) Transwell assay was used to detect the cell invasion (**H**) Cell migration number of NC and NXF3 shRNA2 groups. **I** Wound healing assay was performed to explore the cell migration. **J** Area wound healed (%) of NC and NXF3 shRNA2 groups. * $P<0.05$, ** $P<0.01$, *** $P<0.001$.

Statistical analysis

Statistical analyses were carried out using GraphPad Prism 8.0. The data summary was presented as mean ± standard deviation (SD) and obtained from at least three independent experiments that were each performed in triplicate. Paired Student's t-test or ANOVA was employed for analysis with multiple comparisons. $P<0.05$ is considered statistically significant.

Results

NCTP model effectively evaluates the prognosis of gastric cancer patients

A total of 105 NCTPs were obtained by retrieving the Nucleocytoplasmic transport (NCT) pathway gene set from the KEGG pathway database. Firstly, Univariate regression analysis was used to evaluate the relationship between these 105 NCTPs and the prognosis of GC patients, revealing that 9 NCTPs are closely associated with the prognosis of GC patients (Fig. 1A and Supplementary Fig. 1), including NXF3, RANGAP1, THOC2, NUP85, NDC1, GLE1, NUP62, NUP43, and NUP50. To further reduce gene numbers in the model, LASSO regression analysis was conducted on these 9 NCTPs (Fig. 1B). Subsequently, 3 NCTPs-related prognosis risk model was constructed, where NXF3 was identified as a high-risk gene, while GLE1 and RANGAP were protective genes. Risk score curve, three-point survival distribution graph, and heatmap of prognosis-related NCTPs was plotted using R software (Fig. 1C). Kaplan–Meier survival analysis demonstrated that the high-risk group had significantly lower survival rates than the low-risk group in the training set (P = 0.0022) (Fig. 1D and F). Finally, ROC curves verified that NCTP-related prognostic risk model can effectively evaluate the prognosis of gastric cancer patients (Fig. 1E).

Next, we downloaded the GEO datasets GSE62254 and GSE84437 to validate the NCTP model; risk score curve, three-point survival distribution graph, and heatmap of prognosis-related nuclear transport proteins were validated and plotted using R software in the GSE84437 (Supplementary Fig. 2A) and GSE62254 (Supplementary Fig. 2D). Kaplan–Meier survival analysis showed the low-risk group has higher survival rates than the high-risk group in the GSE84437 (Supplementary Fig. 2B) and GSE62254 (Supplementary Fig. 2E). ROC curves verified that NCTP-related prognostic risk model can effectively evaluate the prognosis of gastric cancer patients in the GSE84437 (Supplementary Fig. 2C) and GSE62254 (Supplementary Fig. 2F). The above result suggested that NCT is a key process related to gastric cancer progression.

High-expression of NXF3 predicts poor prognosis in gastric cancer

Next, we sought to identify key NCTP that influence the malignant progression of gastric cancer, and analyzed the differential expression of these 105 NCTPs in gastric cancer tissues and adjacent tissues. As shown in Fig. 2A, the heatmap displays 11 differentially expressed NCTPs in between gastric cancer tissues and adjacent tissues, including 11 significantly increased NCTPs (NXF3, NUP210L, POM121L2, NUP107, RANBP17, IPO4, KPNA2, NDC1, XPO5, NUP155, CSE1L) and 0 significantly decreased NCTP. We intersected the differentially expressed NCTP with the 9 prognosis-related NCTP, and the Venn diagram shows 2 shared NCTP (NDC1 and NXF3) (Fig. 2B). NDC1 is significantly increased in gastric cancer (Fig. 2C), but gastric cancer patients with low NDC1 expression have a shorter overall survival rate compared to those with high NDC1 expression (Fig. 2D). Notably, NXF3 is significantly highly-expressed in gastric cancer, with consistent unfavorable survival rate, indicating that gastric cancer patients with high NXF3 expression have a poor overall survival than those with low NXF3 expression. Additionally, we analyzed the NXF3 protein in gastric cancer tissues using IHC staining through The Human Protein Atlas online database [16], and representative IHC images were shown in Figs. 2E. As shown in Figs. 2F, gastric cancer patients with low NXF3 protein expression shows a longer survival time than those with high NXF3 expression in another dataset of Kaplan–Meier Plotter. Therefore, nuclear transport protein NXF3 is considered a hazardous prognostic marker in gastric cancer.

To determine whether NXF3 expression is an independent prognostic factor, we conducted multivariate Cox regression analysis, adjusting for other clinical variables such as age, gender, lymph node metastasis, M stage, N stage, T stage, Stage (Table 3). The results showed that NXF3 expression, age > 60 years, and lymph node metastasis (≥ 3 positive nodes) are independent prognostic factors for gastric cancer patients in this analysis. M1stage is a strong predictor

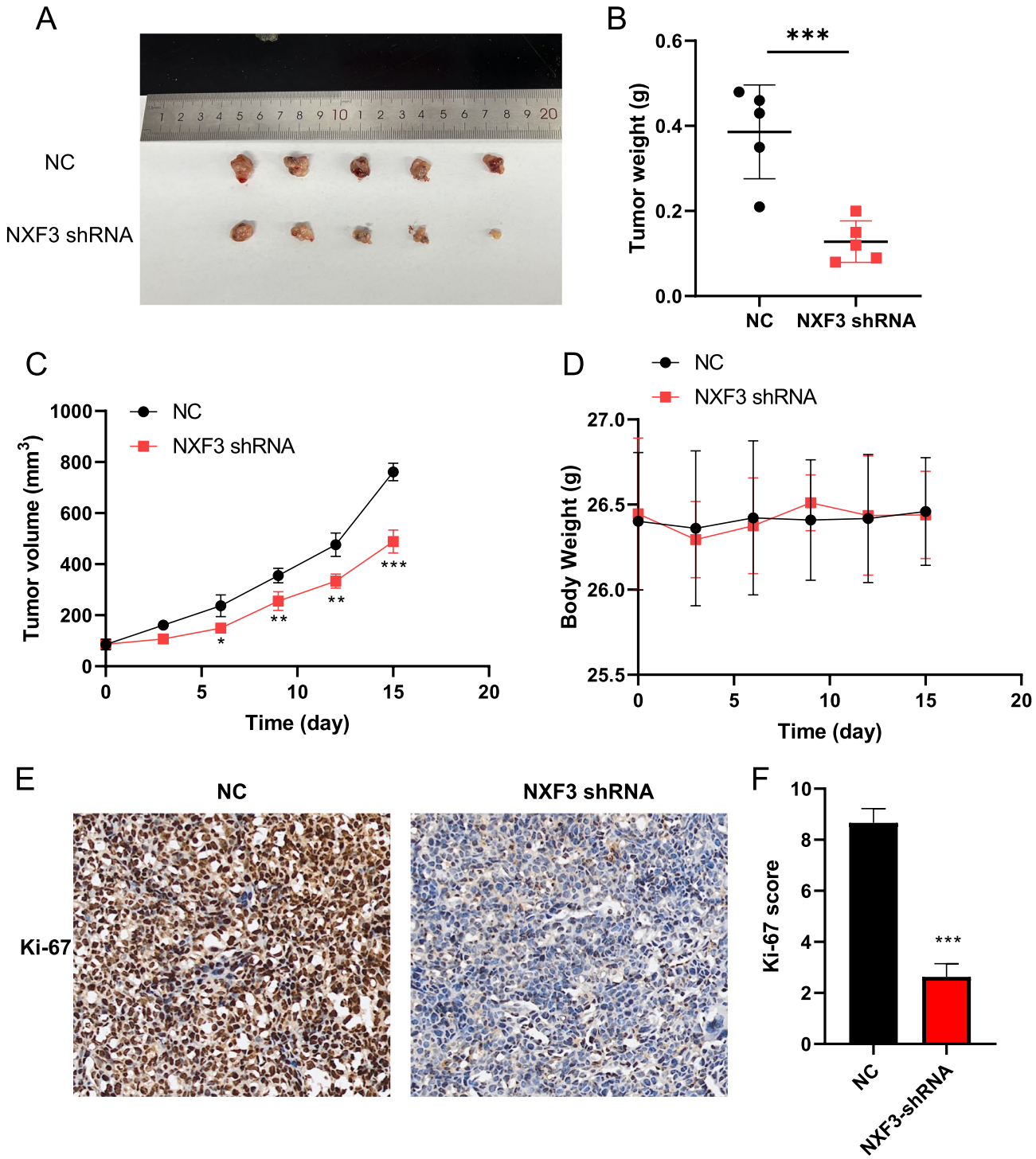

Fig. 4 Silencing NXF3 inhibited GC cell growth in vivo. **A** Morphological images of mice and harvested tumors in both groups (n = 5); **B** Tumor weight was determined in both groups (n = 5); **C** The tumor volume was measured every 3 days (n = 5); **D** The mice body weight was determined in both groups (n = 5); **E** Ki-67 protein expression was detected in both groups by IHC staining; **F** Statistical analysis of Ki-67 protein IHC score in both groups. * $P < 0.05$, ** $P < 0.01$, *** $P < 0.001$

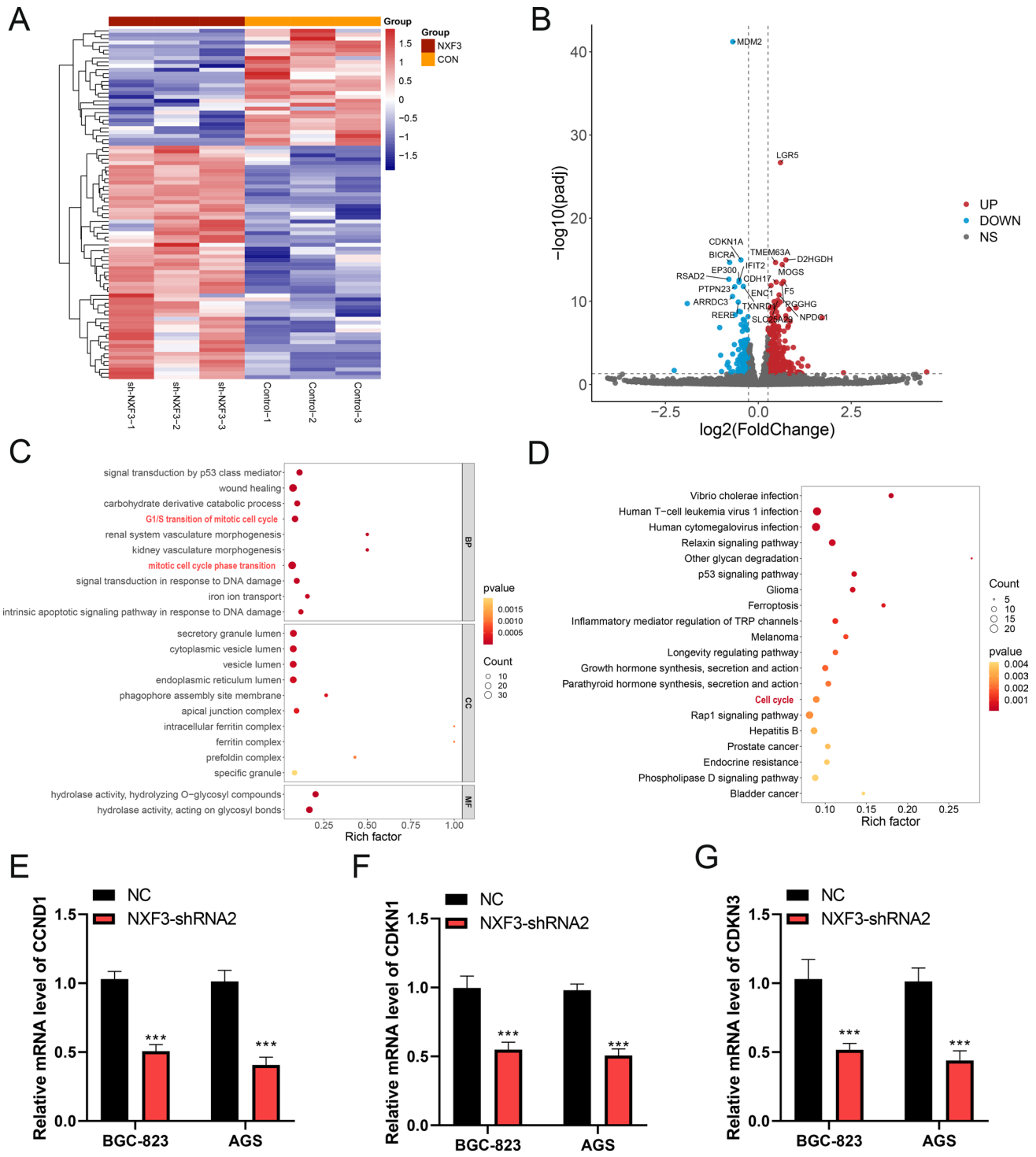

Fig. 5 NXF3 regulated cell cycle in GC cells. **A** Heat map showing differentially expressed genes in the sh-NXF3 and control groups, with red representing significantly increased genes and blue representing significantly decreased genes; **B** Volcano plot displaying the top 10 increased or decreased genes between the sh-NXF3 group and control group; **C** Functional enrichment analysis of differentially expressed genes, including Biological Processes (BP), Cellular Components (CC), and Molecular Functions (MF); **D** Enrichment analysis of KEGG signaling pathways for downstream differentially expressed genes of NXF3; (**E**–**G**) RT-qPCR assay was used to detect the mRNA level of CCND1(**E**), CDKN1(**F**), and CDKN3(**G**) in NC and NXF3-shRNA2 groups of BCG-823 and AGS cells. * $P<0.05$, ** $P<0.01$, *** $P<0.001$

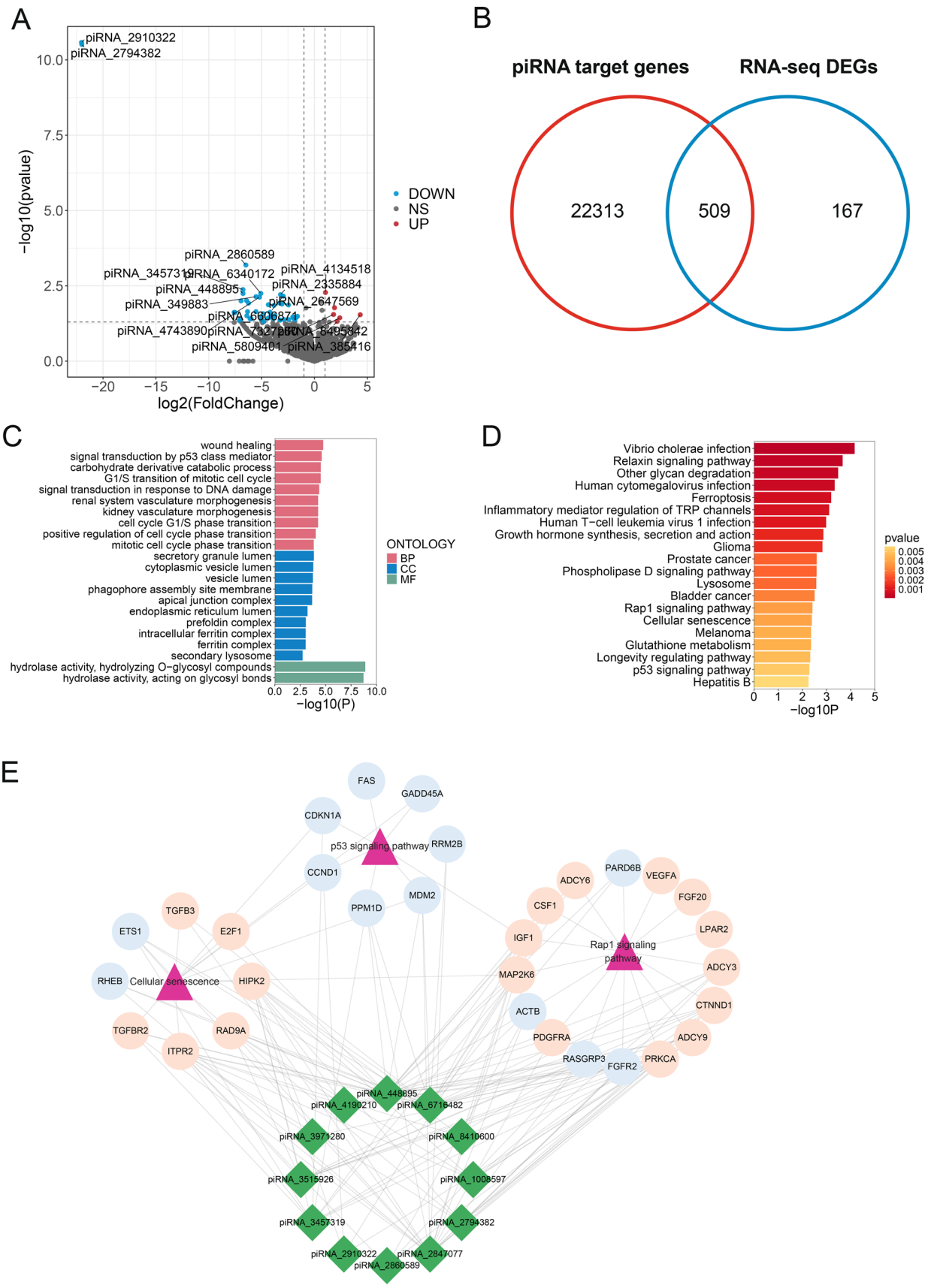
A
piRNA_2910322
piRNA_2794382
piRNA_2860589
piRNA_3457319
piRNA_6340172
piRNA_4134518
piRNA_448895
piRNA_2335884
piRNA_349883
piRNA_2647569
piRNA_6006874
piRNA_4743890
piRNA_8495842
piRNA_5809401
piRNA_385416
DOWN
NS
UP
−log10(pvalue)
log2(FoldChange)
B
piRNA target genes
RNA-seq DEGs
22313
509
167
C
wound healing
signal transduction by p53 class mediator
carbohydrate derivative catabolic process
G1/S transition of mitotic cell cycle
signal transduction in response to DNA damage
renal system vasculature morphogenesis
kidney vasculature morphogenesis
cell cycle G1/S phase transition
positive regulation of cell cycle phase transition
mitotic cell cycle phase transition
secretory granule lumen
cytoplasmic vesicle lumen
vesicle lumen
phagophore assembly site membrane
apical junction complex
endoplasmic reticulum lumen
prefoldin complex
intracellular ferritin complex
ferritin complex
secondary lysosome
hydrolase activity, hydrolyzing O−glycosyl compounds
hydrolase activity, acting on glycosyl bonds
ONTOLOGY
BP
CC
MF
−log10(P)
D
Vibrio cholerae infection
Relaxin signaling pathway
Other glycan degradation
Human cytomegalovirus infection
Ferroptosis
Inflammatory mediator regulation of TRP channels
Human T−cell leukemia virus 1 infection
Growth hormone synthesis, secretion and action
Glioma
Prostate cancer
Phospholipase D signaling pathway
Lysosome
Bladder cancer
Rap1 signaling pathway
Cellular senescence
Melanoma
Glutathione metabolism
Longevity regulating pathway
p53 signaling pathway
Hepatitis B
pvalue
−log10P
E
FAS
GADD45A
CDKN1A
p53 signaling pathway
RRM2B
CCND1
MDM2
PPM1D
TGFB3
ETS1
E2F1
RHEB
Cellular senescence
HIPK2
TGFBR2
RAD9A
ITPR2
PARD6B
VEGFA
ADCY6
FGF20
CSF1
LPAR2
IGF1
Rap1 signaling pathway
ADCY3
MAP2K6
CTNND1
ACTB
ADCY9
PDGFRA
PRKCA
RASGRP3
FGFR2
piRNA_448895
piRNA_4190210
piRNA_6716482
piRNA_3971280
piRNA_8410600
piRNA_3515926
piRNA_1008597
piRNA_3457319
piRNA_2794382
piRNA_2910322
piRNA_2847077
piRNA_2860589

◂**Fig. 6** piRNA sequencing and functional enrichment analysis of target genes of piRNAs. **A** Volcano plot displaying the significantly increased or decreased piRNAs between the sh-NXF3 group and control group; **B** Venn diagram shown a total of 509 NXF3-regulated target genes through piRNAs regulation; **C** Functional enrichment analysis of differentially expressed genes, including Biological Processes (BP), Cellular Components (CC), and Molecular Functions (MF); **D** Enrichment analysis of KEGG signaling pathways for downstream differentially expressed genes of NXF3; **E** piRNAs-target genes-signaling pathway network was created

of poor prognosis. Other factors such as gender, N stage, T stage, and overall stage did not show significant associations with prognosis in this multivariate analysis. This finding suggests that NXF3 can serve as a robust biomarker for predicting clinical outcomes in GC.

NXF3 knockdown represses gastric cancer malignant properties and tumor growth in vitro *and* in vivo

The function of NXF3 in gastric cancer remains unclear and requires further investigation. First, we transfected three shRNAs (shRNA1, shRNA2 and shRNA3) into gastric cancer cell lines AGS and BCG-823. As a result, RT-qPCR assays indicated that shRNA2 displayed the most significant efficiency for NXF3 knockdown among BGC-823 and AGS cells (Fig. 3A). Moreover, the efficiency of NXF3 knockdown was validated using Western blot analysis. WB results showed a significant reduction in NXF3 protein levels in NXF3 shRNA2 groups compared to NC, shRNA1, and shRNA3 groups of BGC-823 and AGC cells (Supplementary Fig. 3A and 3B). The malignant properties of NXF3 knockdown were evaluated with various cell assays. Knockdown of NXF3 resulted in significant inhibition of the proliferation of BGC-823 and AGC cells, as evidenced by the CCK-8 assay (Fig. 3B, C). The effect of NXF3 on apoptosis was then analyzed using flow cytometry, revealing that its knockdown induced higher rates of cell apoptosis (15.93% vs 4.98%) in BGC-823 cell and (9.68% vs 4.24%) in AGS cell (Fig. 3D). Flow cytometry analysis was performed to determine effect of NXF3 knockdown on cell cycle arrest. As a result, knocking down NXF3 with shRNA significantly reduced the percentage of cells in the G0/G1 phase and increased the percentage of cells in the G2/M phase in both BGC-823 (Fig. 3E) and AGS cells (Fig. 3F). Furthermore, the results of the transwell and wound healing assays exhibited that compared to the control group, the invasion and migration capabilities of cells in the NXF3 shRNA2 group are reduced (Fig. 3G–J). Collectively, these results revealed that NXF3 acts as an oncogene in vitro for gastric cancer.

To confirm the *in-vitro* effects, we studied the effect of NXF3 silencing on tumor growth by inducing tumor formation in nude BALB/c mice through subcutaneous injection of tumor cells. The mice were randomly divided into two groups: the control group (NC) and the group with stable transfection of NXF3 shRNA into AGS cells. Tumor size, volume, and weight of the mice in each group were measured to assess tumor growth. Compared to the control group, tumor growth was significantly decreased in the NXF3 shRNA group (Fig. 4A). There was no significant difference in the body weight change of the mice between the two groups, which may indicate that NXF3 shRNA treatment had minimal impact on the overall health and physiological status of the mice (Fig. 4B). The results of plotting the tumor growth curve indicated NXF3 shRNA significantly inhibited tumor growth compared to the control group (Fig. 4C). Tumor size was significantly reduced in the NXF3 shRNA group compared to the control group (Fig. 4D). Next, Ki-67 protein (a cell proliferation marker related to cell cycle [17]) expression was detected by IHC staining, and NXF3 silencing significantly inhibited Ki-67 expression (Fig. 4E and F). These results suggested that silencing of the NXF3 gene showed a significant inhibitory effect on tumor growth, and provides evidence for potential tumor therapy strategies targeting the NXF3 in GC.

NXF3 regulates the cell cycle and oncogenic pathways

The above functional and phenotype of NXF3 paves us to explore the underlying mechanism of NXF3 in gastric cancer. In order to explore the impact of NXF3 silencing on tumor related pathways, we knocked down NXF3 in AGS cells and conducted RNA-Seq to detect changes in downstream gene expression, followed by biological pathway and functional enrichment analysis. The heatmap shows significantly differentially expressed genes in between the control group and the sh-NXF3 group (Fig. 5A). The volcano plot displays the top 10 significantly increased and decreased genes in AGS cells of the control group and sh-NXF3 group (Fig. 5B). Subsequently, differentially expressed genes (DEGs) were subjected to GO functional enrichment analysis, showing that NXF3 impacts the biological processes of mitotic cell cycle G1/S transition, wound healing, mitotic cell cycle phase transition and intrinsic apoptotic signaling pathway in response to DNA damage (Fig. 5C). KEGG pathway enrichment analysis indicated that NXF3 affects the cell cycle, p53 signaling pathway, ferroptosis and Rap1 signaling pathway (Fig. 5D). Furthermore, RT-qPCR assay confirmed that NXF3 decreased the cell cycle related genes (CCND1, CDKN1, and CDKN3) mRNA level in BGC-823 and AGS cells (Fig. 5E-5J). Above results revealed that NXF3 promotes the malignant progression of gastric cancer by influencing cell cycle related pathways.

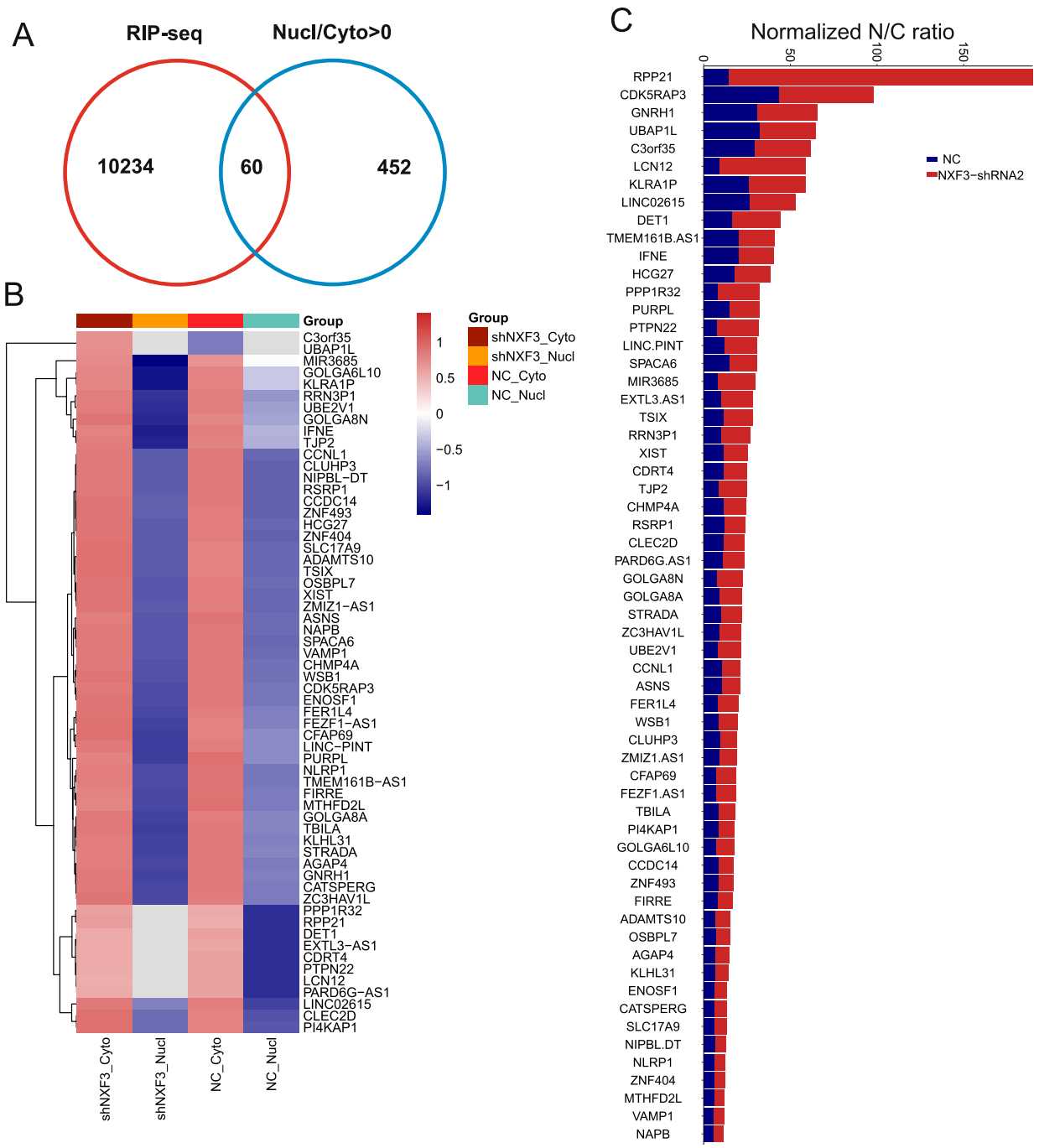

Fig. 7 RIP-Seq and nuclear-cytoplasmic RNA-Seq reveals NXF3 binding RNAs. **A** The Venn diagram shows the intersection of genes with RIP-Seq and Nuclear/Cytoplasmic > 0 **B** The heatmap illustrates the expression of genes regulated by NXF3 in the nucleus and cytoplasm of the control group and shNXF3 group; **C** The nuclear-cytoplasmic ratio changes of genes regulated by NXF3 in the control and shNXF3 groups

NXF3 modulates cellular senescence related oncogenic pathways via piRNA-target network

Researchers have discovered that NXF3 can bind to RNAs and participate in abnormal nuclear-cytoplasmic translocation [18], in which piRNA is regulated by NXF3 during spermatogenesis. However, it is unknown whether NXF3 affects piRNA in tumors. To elucidate the role of NXF3 in gastric cancer through piRNA regulation, we conducted piRNA sequencing and mRNA sequencing. First, a total of 53 differentially expressed piRNAs were identified between NC and sh-NXF3 groups of AGS cells (Fig. 6A).

Notably, several piRNAs were significantly upregulated (e.g., piRNA_4134518, piRNA_2647569) and downregulated (e.g., piRNA_3457319, piRNA_448895) in response to NXF3 knockdown. To explore the functional impact of these differentially expressed piRNAs, we predicted their downstream target genes and intersected these with differentially expressed genes from RNA-seq analysis. The Venn diagram showed a total of 509 target genes regulated by NXF3 through piRNA-mediated mechanisms (Fig. 6B). GO function enrichment analysis indicated that the piRNA-regulated target genes were enriched in pathways related to tumor cell proliferation, migration, and other processes (Fig. 6C). Specifically, the tope enriched terms included the BP of Cell cycle progression, DNA damage response, and cellular senescence, and the CC of Nucleus, cytoplasmic vesicles, and mitochondria. KEGG pathway enrichment analysis revealed that piRNA-regulated target genes were enriched in RAP1 signaling pathway, Cellular senescence, and p53 signaling pathway (Fig. 6D). Furthermore, we constructed a network of piRNA-target genes-signaling pathways (Fig. 6E). Notably, oncogenic pathways related mRNAs and piRNAs were enriched, including piRNA_3457319-CCND1/CDKN1A-p53 signaling pathway, piRNA_2847077-TGFB3/TGFBR2-Cellular senescence, piRNA_448895-IGF1/PDGFRA/ACTB/MAP2K6-Rap1 signaling pathway.p53 Signaling Pathway: Key genes such as CCND1 and CDKN1A were identified as potential targets of piRNA_3457319, which is regulated by NXF3. Rap1 Signaling Pathway: Genes like IGF1, PDGFRA, ACTB, and MAP2K6 were found to be regulated by piRNA_448895. Cellular Senescence Pathway: piRNA_2847077 was shown to target TGFB3 and TGFBR2, which are critical for cellular senescence. These findings suggest that NXF3 modulates oncogenic pathways in gastric cancer by regulating the expression and function of piRNAs, which in turn target key genes involved in cell cycle progression, cellular senescence, and apoptosis.

NXF3 functions in gastric cancer cells by affecting RNA export

NXF3 is a nuclear RNA export factor, involved in the transportation of mRNA (messenger RNA) and other small RNA molecules from the nucleus to the cytoplasm. Next, we conducted RIP-Seq analysis to investigate the mRNA interacting with NXF3 protein. The RIP-Seq results revealed that a total of 10,294 RNAs interacting with NXF3 (Fig. 7A**,** Table 1). Furthermore, we utilized nuclear-cytoplasmic transcriptomics to study the impact of NXF3 knockdown on RNA localization inside the cell. The nuclear-cytoplasmic transcriptomics results showed that the knockdown of NXF3 significantly increased 512 genes mRNA nuclear retention (Fig. 7A**,** Table 2), suggesting an impact of NXF3 in RNA nuclear-cytoplasmic transportation. By intersecting the RIP-Seq and nuclear-cytoplasmic transcriptomics results, we identified 60 genes whose mRNA nuclear retention was influenced by NXF3. The heatmap illustrates the expression of these 60 genes in the nucleus and cytoplasm of both the control group and the sh-NXF3 group (Fig. 7B). Changes of the 60 genes nuclear-cytoplasmic ratio are depicted in Fig. 7C, including RPP21, CDK5RAP3, GNRH1, LCN12 and etc.

To rule out the possibility of NXF3 regulating the cell cycle and gastric cancer progression through protein interactions, we identified proteins binding to NXF3 through immunoprecipitation followed by mass spectrometry. The results showed that there were only 4 proteins specifically binding to NXF3 compared to IgG (Table 3), including LUC7L, RACK1, LMNA, and SMTN. These proteins show weak signals with NXF3 binding. IP-MS confirmed that NXF3 functions by affecting RNA output through its influence on RNA-binding protein domains.

NXF3 promotes cell cycle progression via nuclear export of CDK5RAP3 mRNA

The above results indicate that NXF3 promotes the malignant progression of gastric cancer by influencing the RNA nuclear export of RPP21, CDK5RAP3 and etc. We found that the expression of CDK5RAP3 is reduced in gastric cancer tissues (Fig. 8A) and correlates with poor prognosis in gastric cancer patients (Fig. 8B). GSEA functional enrichment analysis shows that CDK5RAP3 regulates the cell cycle (Fig. 8C). CDK5RAP3 (also known as CDK5 regulatory subunit-associated protein 3 or Interacting protein of CDK5 and CDK5RAP3) is a protein associated with cell cycle regulation and cell proliferation. To verify the effect of NXF3 on CDK5RAP3 mRNA nuclear export, RT-qPCR validated a significant increase in CDK5RAP3 mRNA nuclear export after NXF3 knockdown in BCG-823 and AGS cells (Fig. 8D). RIP-Seq results demonstrated the binding interaction of NXF3 protein with CDK5RAP3 mRNA (Fig. 8E). RIP-qPCR confirmed the interaction between NXF3 protein and CDK5RAP3 mRNA (Fig. 8F).

Furthermore, we further examined the impact of overexpressing CDK5RAP3 on cell proliferation and cell cycle proportions in BCG-823 and AGS cells. Firstly, RT-qPCR assay and Western blot assay validated the successful transfection of overexpressed CDK5RAP3 in BCG-823 and AGS cells (Fig. 8G and supplementary Fig. 4). CCK-8 assay results showed that overexpression of CDK5RAP3 significantly inhibited cell proliferation in BCG-823 and AGS cells (Fig. 8H-I). FACS analysis revealed that CDK5RAP3 is involved in cell cycle regulation, especially at the G1/S and G2/M transition points, affecting cell proliferation and division (Fig. 8J–K). In summary, NXF3

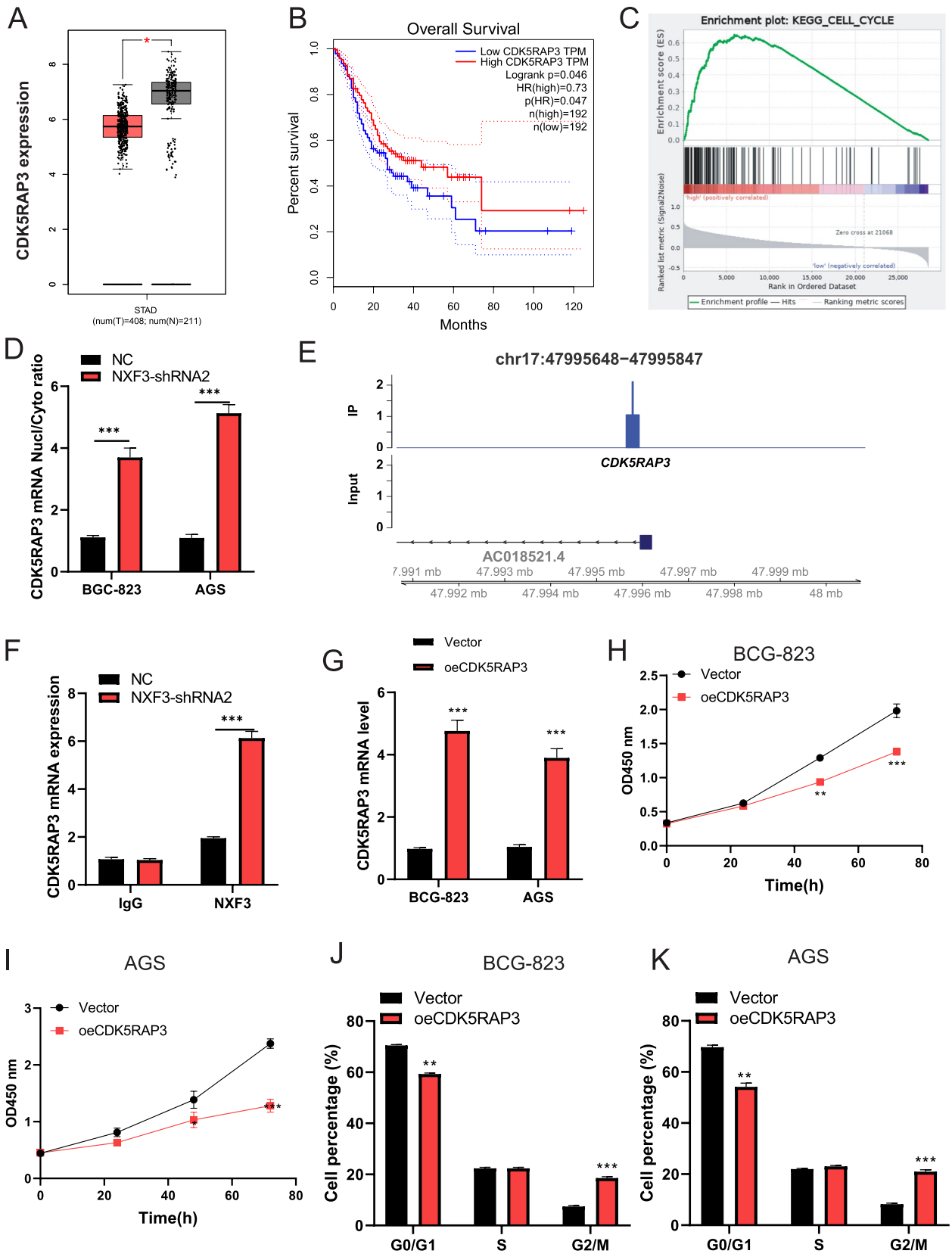
A
CDK5RAP3 expression
STAD
(num(T)=408; num(N)=211)
B
Overall Survival
Low CDK5RAP3 TPM
High CDK5RAP3 TPM
Logrank p=0.046
HR(high)=0.73
p(HR)=0.047
n(high)=192
n(low)=192
Percent survival
Months
C
Enrichment plot: KEGG_CELL_CYCLE
Enrichment score (ES)
Ranked list metric (Signal2Noise)
Zero cross at 21068
Rank in Ordered Dataset
Enrichment profile
Hits
Ranking metric scores
D
NC
NXF3-shRNA2
CDK5RAP3 mRNA Nucl/Cyto ratio
BGC-823
AGS
E
chr17:47995648−47995847
IP
Input
CDK5RAP3
AC018521.4
F
NC
NXF3-shRNA2
CDK5RAP3 mRNA expression
IgG
NXF3
G
Vector
oeCDK5RAP3
CDK5RAP3 mRNA level
BCG-823
AGS
H
BCG-823
Vector
oeCDK5RAP3
OD450 nm
Time(h)
I
AGS
Vector
oeCDK5RAP3
OD450 nm
Time(h)
J
BCG-823
Vector
oeCDK5RAP3
Cell percentage (%)
G0/G1
S
G2/M
K
AGS
Vector
oeCDK5RAP3
Cell percentage (%)
G0/G1
S
G2/M

◂**Fig. 8** NXF3 promotes gastric cancer progression by nuclear transport of CDK5RAP3 mRNA and the cell cycle. CDK5RAP3 expression in GC tissues and normal tissues from the TCGA database; **A** CDK5RAP3 expression was associated with overall survival of 384 patients with GC from the TCGA database; **B** GSEA of Cell cycle up GSEA gene sets referred to as cell cycle related gene signatures; NES, normalized enrichment score; **C** The levels of nuclear and cytoplasmic CDK5RAP3 mRNA were determined by RT-qPCR assay; **D** RIP-Seq assay showed that NXF3 interacted with CDK5RAP3 in GC cells; **E** RIP-qPCR verified that NXF3 interacted with CDK5RAP3 in GC cells; **F** The mRNA expression of CDK5RAP3 was detected by using RT-qPCR; G (H-I) CCK-8 assay was used to explore the effect of OE-CDK5RAP3 on the proliferation of BGC-823 and AGS cells. **J**–**K** Cell cycle detection was used to analysis the proportion of cells in G0/G1 phase, S phase, and G2/M phase; *$P<0.05$; ** $P<0.01$, *** $P<0.001$

promotes the malignant progression of gastric cancer cells by affecting the nuclear export of CDK5RAP3 mRNA and consequently influencing the cell cycle.

Collectively, the above results showed that after NXF3 silencing, there were 53 differential piRNAs, and their target genes and functions are related to the P53 signaling pathway, Cell cycle, Rap1 signaling pathway and cell senescence (Fig. 9).

Discussion

Gastric cancer is a highly malignant tumor with high invasiveness, high recurrence rate, and poor prognosis [19]. Early identification of adverse prognostic factors and targeted personalized treatments are crucial for improving survival rates, necessitating more sensitive and reliable biomarkers [20]. This study systematically analyzed the role of nuclear-cytoplasmic transport proteins (NCTPs) in gastric cancer (GC) and identified NXF3 as a key regulator of GC progression. Our findings highlight the potential of NXF3 as a therapeutic target and biomarker for GC, with significant clinical and scientific implications.

Through Univariate analysis, nine NCTPs associated with the prognosis of gastric cancer patients were identified (NUP85, NUP50, RANGAP1, THOC2, NXF3, GLE1, NUP62, and NDC1). A risk scoring model containing three nuclear-cytoplasmic transport genes, including RANGAP1, GLE1, NXF3, was constructed. Kaplan–Meier survival analysis shows that the risk score can effectively predict the prognosis of gastric cancer patients. Low expression of NUP85 and NUP43 are significantly associated with poor prognosis in gastric cancer [21, 22]. RanBP2 acts as SUMO E3 ligase to promote nuclear-plasma transport via combining with RanGAP1 in gastric cancer [23]. knockdown of THOC2 inhibited the growth and metastatic behaviors of GC cells [24]. Nup62 is a member of the nuclear pore complex (NPC), NUP62 was increased in GC and related poor prognosis, NUP62 promoted metastasis of GC by regulating Wnt/β-Catenin and TGF-β signaling pathways [25]. In summary, we consider abnormal nuclear-cytoplasmic translocation to be a key pathway in the occurrence and development of gastric cancer.

In eukaryotic cells, the transport of macromolecules in the nucleus-cytoplasm is strictly controlled by NCTPs, importins, and exportins [26]. These proteins serve as transport receptors and promote normal transport by binding to their cargo through specific nuclear localization signals or nuclear export signals (NLS/NES) [27]. Compared to normal cells, malignant tumors often overexpress specific importins and/or exportins, as the maintenance of the abnormally high growth rate of cancer cells requires additional transport demands [28]. Therefore, disrupting the function of key nuclear-cytoplasmic transport proteins, preventing cancer proteins from being imported into the nucleus, or anti-cancer proteins from being exported out of the nucleus, represents a promising strategy for developing new cancer treatment methods. Our study constructed a prognostic risk model based on NCTPs, including NXF3, which effectively predicts the prognosis of GC patients. The high expression of NXF3 is associated with poor overall survival, suggesting its potential as a prognostic biomarker. This could aid clinicians in stratifying patients into high-risk and low-risk groups, thereby informing treatment decisions and improving patient management. Ki-67 is a cell proliferation marker, and its expression in the cell cycle is closely related to the cell division cycle [17]. The positivity rate of Ki-67 can reflect the proliferative activity of tumor cells. The higher the positivity rate, the faster the growth rate of tumor cells, indicating a higher degree of malignancy and invasiveness of the tumor. Next, Ki-67 protein expression was detected by IHC staining; NXF3 silencing significantly inhibited Ki-67 protein expression NXF3 plays an oncogenic role in gastric cancer, and targeting NXF3 holds promise as a new therapeutic target for treating gastric cancer. The functional experiments in vitro and in vivo demonstrated that NXF3 knockdown significantly inhibits GC cell proliferation, migration, invasion, and tumor growth. These results suggest that targeting NXF3 could be a novel therapeutic strategy for GC.

NXF3 is a member of the nuclear RNA export factor family, which is involved in the nuclear export processes of various RNAs [11, 13]. NXF3 has been identified as a novel germ cell-specific export adapter for unsliced piRNA precursors, revealing its role in the transport process from transcription sites to cytoplasmic piRNAs biogenesis sites [12]. Additionally, we also discovered that NXF3 regulates piRNAs [14]. In order to preliminarily explore the impact of NXF3 silencing on tumor-related pathways, we conducted RNA-Seq and found that NXF3 regulated G1/S transition of the mitotic cell cycle, wound healing, mitotic cell cycle

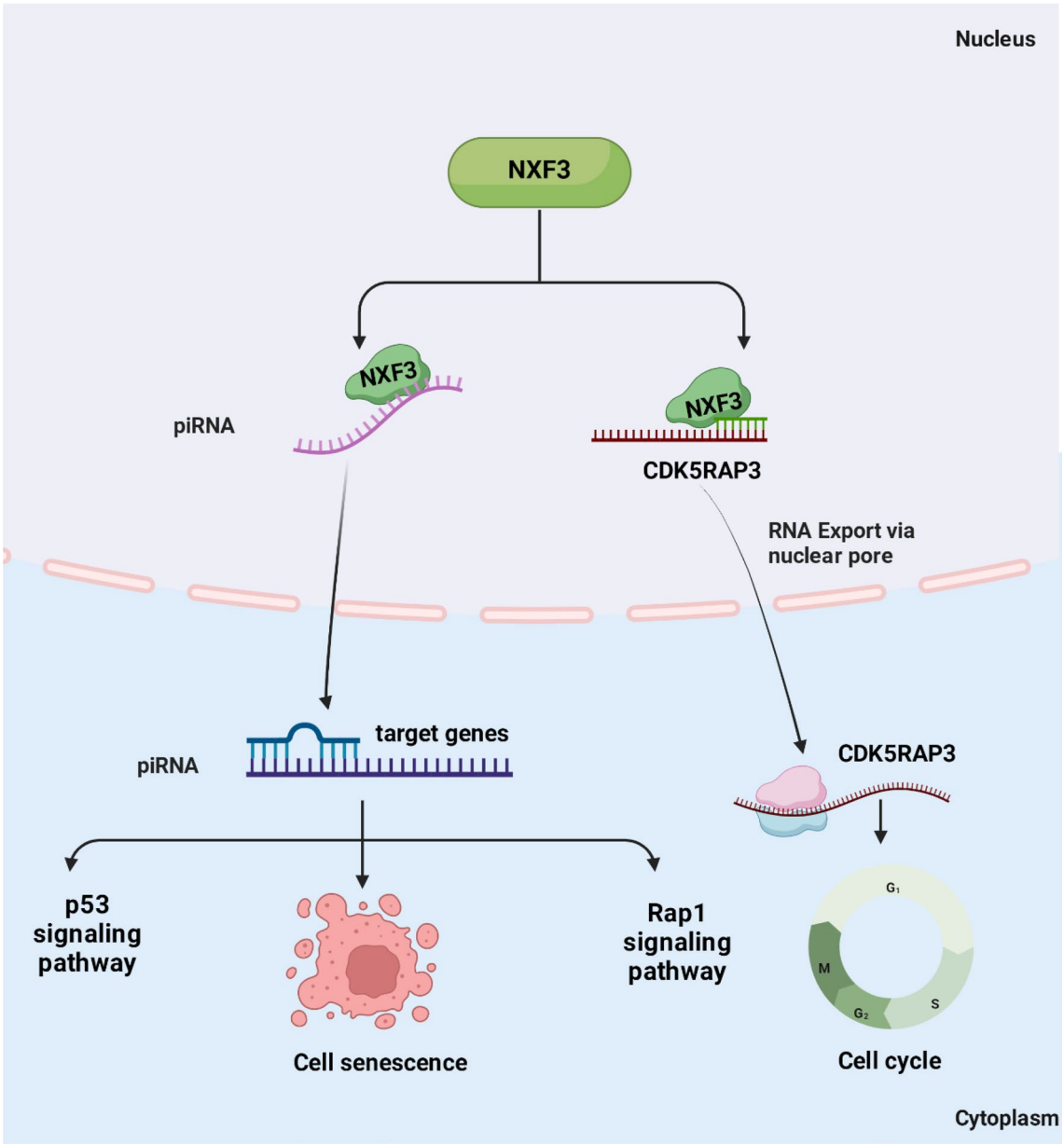

Fig. 9 A schematic model for the potential roles of the NXF3 in gastric cancer. On one hand, the high expression of NXF3 regulates the transport of piRNAs, thereby affecting cell senescence, the p53 signaling pathway, and the Rap1 signaling pathway; on the other hand, NXF3 binds to CDK5RAP3 RNA, promoting its nuclear translocation to influence cell cycle progression

phase transition, cell cycle, p53 signaling pathway, Ferroptosis, Rap1 signaling pathway. NXF3 regulated genes by related oncogenic pathway in GC. Research has found that NXF3 can bind to RNA and participate in abnormal nuclear-cytoplasmic translocation, where piRNAs are regulated by NXF3 in sperm development, but it is unclear whether there are changes in tumors. Therefore, we conducted two analyses, one for piRNA sequencing and the other for mRNA sequencing.

Changes of cell cycle are one of the key steps in the occurrence and progression of tumors [29]. Disruption of the cell cycle can lead to carcinogenesis. Some characteristics of tumor cells, such as unlimited proliferation, self-sufficiency in growth, and insensitivity to growth inhibitory signals, may be a direct result of cell cycle deregulation [30, 31]. In exploring how NXF3 influences the malignant progression of gastric cancer, an interesting finding is that downstream genes of NXF3 are significantly enriched in cell cycle-related signaling pathways. Additionally, in this study, silencing of NXF3 in gastric cancer cells resulted in cell cycle arrest as detected by cell cycle analysis. CDK5RAP3 is a protein related to cell

cycle regulation [32]. CDK5RAP3 plays an important role in the cell cycle, especially in cell growth, mitosis, and cell death [33]. Studies have shown that CDK5RAP3 is widely distributed in the centrosome, spindle apparatus, and endoplasmic reticulum, participating in the regulation of various cellular activities [34]. When CDK5RAP3 is underexpressed, the cell cycle is partially halted in the G2/M phase, leading to a decrease in cell proliferation rate, but this cell cycle arrest does not induce apoptosis [35]. We found that NXF3 promotes the malignant progression of gastric cancer cells by influencing the nuclear export of CDK5RAP3 mRNA, thus affecting the cell cycle.

In conclusion, the abnormal nuclear-cytoplasmic translocation of RNA and proteins is a key molecular event in the progression of gastric cancer. NXF3 induces malignant proliferation and invasive migration of tumor cells with mechanisms related to its RNA binding and RNA transport activities. Specifically, the overexpression of NXF3 regulates piRNAs transport, leading to increased expression of genes involved in apoptosis, the cell cycle, invasion, and migration. Additionally, the binding of NXF3 to CDK5RAP3 RNA activates its nuclear export transition, resulting in excessive cell proliferation and promoting gastric cancer progression. Therefore, targeting NXF3 could inhibit these effects and have potential therapeutic value in treating gastric cancer.

Although studies have revealed the influence of NXF3 on cell cycle and gastric cancer progression through the piRNA-related pathway and nucleocytoplasmic transport of CDK5RAP3 mRNA, the specific molecular mechanisms and detailed roles of signaling pathways still require further investigation. Our study primarily focused on the short-term effects of NXF3 on gastric cancer cells in vitro and in vivo, but long-term efficacy and safety assessments have not yet been conducted. While NXF3 has been identified as a potential target for gastric cancer treatment, its feasibility, safety, and efficacy in clinical applications need validation through large-scale clinical trials. In the future, the discovery of the mechanism of action of NXF3 as a nucleocytoplasmic transport protein in gastric cancer may provide opportunities for developing new treatment strategies, especially targeted therapy against NXF3. The discovery of NXF3 and its related piRNAs and mRNAs provides an opportunity to develop new biomarkers, which may aid in the early diagnosis and prognosis assessment of gastric cancer.

Supplementary Information The online version contains supplementary material available at https://doi.org/10.1007/s00018-025-05630-y.

Acknowledgements None.

Author contributions Cheng Zhang: Conceptualization, Methodology, study design and interpretation of data. Dongyang Wang: analysis of the data. Yuanruohan Zhang, Yuguang Shen: made the figures. Jiahua Liu: Writing original draft. All authors critically reviewed the study protocol and manuscript and approved the final manuscript.

Funding The authors have not disclosed any funding.

Data availability All data can be accessed by contacting the corresponding author.

Declarations

Conflict of interest The authors declare that they have no conflict of interest.

Consent for publication No conflict of interest exits in the submission of this manuscript, and manuscript is approved by all authors for publication.

Ethical approval The Animal experiment protocol listed below has been reviewed and approved by Laboratory animal management ethics committee of Renji Hospital (Approval No. 2023031).

References

1. Li GZ, Doherty GM, Wang J (2022) Surgical management of gastric cancer: a review. JAMA Surg 157(5):446–454
2. Ajani J et al (2022) Gastric cancer, version 22022, NCCN clinical practice guidelines in oncology. J Natl Compr Cancer Netw 20(2):167–192
3. Cao Y et al (2022) Latency-associated peptide identifies immunoevasive subtype gastric cancer with poor prognosis and inferior chemotherapeutic responsiveness. Ann Surg 275(1):e163–e173
4. An M et al (2022) Aberrant nuclear export of circNCOR1 underlies SMAD7-mediated lymph node metastasis of bladder cancer. Cancer Res 82(12):2239–2253
5. Ripin N, Parker R (2023) Formation, function, and pathology of RNP granules. Cell 186(22):4737–4756
6. Yang Y et al (2023) Nuclear transport proteins: structure, function, and disease relevance. Signal Transduct Target Ther 8(1):425
7. Rodriguez JA (2014) Interplay between nuclear transport and ubiquitin/SUMO modifications in the regulation of cancer-related proteins. Semin Cancer Biol 27:11–19
8. Wang J et al (2023) Fucoxanthin inhibits gastric cancer lymphangiogenesis and metastasis by regulating Ran expression. Phytomedicine 118:154926
9. Wang F et al (2022) Nup54-induced CARM1 nuclear importation promotes gastric cancer cell proliferation and tumorigenesis

through transcriptional activation and methylation of Notch2. Oncogene 41(2):246–259
10 Sexton R et al (2019) Targeting nuclear exporter protein XPO1/CRM1 in gastric cancer. Int J Mol Sci. https://doi.org/10.3390/ijms20194826
11. Jiang JH et al (2014) Prognostic significance of nuclear RNA export factor 3 in hepatocellular carcinoma. Oncol Lett 7(3):641–646
12. Kneuss E et al (2019) Specialization of the drosophila nuclear export family protein Nxf3 for piRNA precursor export. Genes Dev 33(17–18):1208–1220
13. Li MW et al (2017) Nuclear export factor 3 regulates localization of small nucleolar RNAs. J Biol Chem 292(49):20228–20239
14. Mendel M, Pillai RS (2019) Nxf3: a middleman with the right connections for unspliced piRNA precursor export. Genes Dev 33(17–18):1095–1097
15. Ouafi M et al (2022) Rapid syndromic testing for respiratory viral infections in children attending the emergency department during COVID-19 pandemic in Lille France 2021–2022. J Clin Virol. https://doi.org/10.1016/j.jcv.2022.105221
16. Digre A, Lindskog C (2021) The human protein atlas-spatial localization of the human proteome in health and disease. Protein Sci 30(1):218–233
17. Sobecki M et al (2017) Cell-cycle regulation accounts for variability in Ki-67 expression levels. Cancer Res 77(10):2722–2734
18 ElMaghraby MF et al (2019) A heterochromatin-specific RNA Export Pathway Facilitates piRNA Production. Cell 178(4):964–979
19. Lopez MJ et al (2023) Characteristics of gastric cancer around the world. Crit Rev Oncol Hematol 181:103841
20. Smyth EC et al (2020) Gastric cancer. Lancet 396(10251):635–648
21. Xia R et al (2021) Prognostic value of a novel glycolysis-related gene expression signature for gastrointestinal cancer in the Asian population. Cancer Cell Int 21(1):154
22. Yang Y et al (2022) In silico development and validation of a novel glucose and lipid metabolism-related gene signature in gastric cancer. Transl Cancer Res 11(7):1977–1993
23. Chen C et al (2020) Opposing biological functions of the cytoplasm and nucleus DAXX modified by SUMO-2/3 in gastric cancer. Cell Death Dis 11(7):514
24. Gu XJ et al (2022) MiR-30e-3p inhibits gastric cancer development by negatively regulating THO complex 2 and PI3K/AKT/mTOR signaling. World J Gastrointest Oncol 14(11):2170–2182
25. Wang H et al (2021) Nuclear pore complex 62 promotes metastasis of gastric cancer by regulating Wnt/beta-catenin and TGF-beta signaling pathways. J Environ Pathol Toxicol Oncol 40(2):81–87
26. Azizian NG, Li Y (2020) XPO1-dependent nuclear export as a target for cancer therapy. J Hematol Oncol 13(1):61
27. Bernhofer M et al (2018) NLSdb-major update for database of nuclear localization signals and nuclear export signals. Nucleic Acids Res 46(D1):D503–D508
28. Hao W et al (2023) hnRNPA2B1 promotes the occurrence and progression of hepatocellular carcinoma by downregulating PCK1 mRNA via a m6A RNA methylation manner. J Transl Med 21(1):861
29. Jamasbi E et al (2022) The cell cycle, cancer development and therapy. Mol Biol Rep 49(11):10875–10883
30. Evan GI, Vousden KH (2001) Proliferation, cell cycle and apoptosis in cancer. Nature 411(6835):342–348
31. Long ZJ et al (2022) cGAS/STING cross-talks with cell cycle and potentiates cancer immunotherapy. Mol Ther 30(3):1006–1017
32. Feng X et al (2022) CDK5RAP3 acts as a putative tumor inhibitor in papillary thyroid carcinoma via modulation of Akt/GSK-3beta/Wnt/beta-catenin signaling. Toxicol Appl Pharmacol 440:115940
33. Yan H et al (2022) CDK5RAP3, an essential regulator of checkpoint, interacts with RPL26 and maintains the stability of cell growth. Cell Prolif 55(5):e13240
34. Quintero M et al (2021) Cdk5rap3 is essential for intestinal paneth cell development and maintenance. Cell Death Dis 12(1):131
35. Zhuo R et al (2024) CDK5RAP3 is a novel super-enhancer-driven gene activated by master TFs and regulates ER-Phagy in neuroblastoma. Cancer Lett 591:216882